



Simultaneous flight control system and twist-morphing wing design of an unmanned aerial vehicle

Bir insansız hava aracının eşzamanlı uçuş kontrol sistemi ve burularak-başkalaşabilen kanat tasarımı

Yüksel Eraslan^{1,*} , Tuğrul Oktay² 

¹ İskenderun Technical University, Aerospace Engineering Department, 31200, Hatay, Türkiye

² Erciyes University, Aircraft Engineering Department, 38039, Kayseri, Türkiye

Abstract

Over the last years, the application of morphing technologies in the aircraft design field has become widespread together with developments in material technologies. In this context, this study discusses the design of an innovative twist-morphing wing on a fixed-wing unmanned aerial vehicle (UAV) aiming to obtain improvement in stall behavior (i.e. stall propagation) and autonomous flight performance. The twist-morphing wing design was designed to be capable of twisting in terms of wash-out angle between 0-degree and 6-degree. In order to have such a multidisciplinary improvement, simultaneous design approach was integrated and SPSA optimization algorithm was used. The washout angle and longitudinal and lateral PID controller coefficients were optimized to have enhancement in autonomous flight performance defined in rise time, settling time and maximum overshoot, which are related with step responses. In result, longitudinal, lateral and total performances were improved by 33.92%, 33.81% and 65.14%, respectively.

Keywords: Aircraft design, Twist-morphing, Autonomous flight performance

1 Introduction

In the field of unmanned aerial vehicles (UAVs), the requirement for enhanced maneuverability and efficiency (i.e. range and endurance) has led to motivate scientists on the development of innovative designs and control systems. In recent years, the conventional aircraft design approaches have witnessed remarkable development via the advancements in material science and technology. In that context, morphing technologies have been one of the most recent innovative applications for the field of aircraft design [1]. Materials such as shape memory alloys or polymers, piezoelectric materials, hybrid materials and electroactive polymers have paved the way for successful morphing capability in aircraft applications [2, 3]. These materials offer advantages over traditional materials in terms of lightweighting, reduced operational costs, improved durability and reliability. In addition, their adaptability and

Öz

Son yıllarda malzeme teknolojilerindeki gelişmelerle birlikte hava aracı tasarımı alanında başkalaşım teknolojilerinin de uygulamaları yaygınlaşmıştır. Bu bağlamda, bu çalışmada, sabit kanatlı bir insansız hava aracı (İHA) üzerinde, perdevites davranışında (yani perdevites yayılımı) ve otonom uçuş performansında iyileşme elde etmeyi amaçlayan yenilikçi bir burularak-başkalaşabilen kanat tasarımı tartışılmaktadır. Burularak-başkalaşabilen kanat tasarımı, 0-derece ile 6-derece arasında burulabilecek şekilde tasarlanmıştır. Böylesi bir multidisipliner iyileştirme için eşzamanlı tasarım yaklaşımı sürece entegre edilmiş ve SPSA optimizasyon algoritması kullanılmıştır. Burulma açısı ile boylamsal ve yanal PID kontrolcü katsayıları, birim basamak tepkisi parametreleri olan yükselme zamanı, yerleşme zamanı ve maksimum aşım ile ifade edilerek otonom uçuş performansında iyileştirme sağlamak için optimize edilmiştir. Sonuç olarak, boylamsal, yanal ve toplam otonom uçuş performanslarının sırasıyla %33.92, %33.81 ve %65.14 oranında iyileştirildiği görülmüştür.

Anahtar kelimeler: Hava aracı tasarımı, Burularak-başkalaşım, Otonom uçuş performansı

flexibility allow designers to create more streamlined and efficient aircraft shapes.

The term “morphing” refers to the ability of an aerial vehicle component to change its shape to obtain an advantage in terms of aerodynamic performance, fuel efficiency, control system performance or similar benefits for an aircraft designer. Such an application could be acted in-flight or pre-flight (on the ground) depending on which one the desired enhancement require. For fixed-wing aircraft, most morphing applications have focused on the main wing and horizontal and vertical tail surfaces, as they are critical to the stability and control of the aircraft. There are various applications in the literature relying on airfoil camber [4, 5], wing taper ratio [6] or sweep angle [7] of the wing. Twist-morphing is another application on the focus of interest aiming for adjusting the stall propagation along the wing, commonly desire to provide start at the root section to avoid stall on control surfaces. The case of the wing root

* Sorumlu yazar / Corresponding author, e-posta / e-mail: yuksel.eraslan@iste.edu.tr (Y. Eraslan)

Geliş / Recieved: 14.06.2024 Kabul / Accepted: 24.07.2024 Yayınlanma / Published: xx.xx.20xx

doi: 10.28948/ngumuh.1501418

section having a higher angle of attack than the tip section is called wash-out, while the opposite is called wash-in.

The deformation of any external component (i.e. morphing) naturally results in multidisciplinary consequences and accordingly affects stability and control issues of an aerial vehicle. Therefore, the application should be drastically investigated and the related effects must be assessed to have an improvement for a beneficial objective. Together with aerodynamical, inertial and geometrical variations due to morphing, from the control point of view, trajectory tracking qualities related with step response of the control system are important for autonomous flight performance of an aerial vehicle. These variables could be mentioned as settling time, rise time and maximum overshoot, and determine the performance of the control system.

Aforesaid multidisciplinary results of the morphing application may require a simultaneous design approach to maximize the benefits of the application. In the conventional design approach, the aerodynamic design and the control system design progresses independently for an aircraft, whereas in the modern approach they are usually integrated and evaluated concurrently. In this regard, an innovative morphing application, such as twist-morphing, on an aircraft could be simultaneously investigated with its control system to maximize the benefits for each discipline.

In the literature, there are various twist-morphing applications aiming for various performance enhancements on aircraft design. For instance, Kaygan and Ulusoy has investigated the performance of twist-morphing wing at various twist angles on Airbus A320 by using Athena Vortex Lattice method and presented the aerodynamic and stability benefits of the application [8]. Ismail et al. has studied twist-morphing on a fixed-wing micro aerial vehicle (MAV) wing and provided an enhanced lift behavior and improved performance [9]. Their assessment integrated with fluid-structure interaction (FSI) and shown the similar enhancement in drag performance. Gatto has investigated a UAV platform to obtain enhanced flight performance with active twist control (i.e. twist-morphing) and improved structural strength [10]. As a result, the glide ratio was found to be significantly improved due to a significant increase in lift and a slight increase in drag. Janett et al. have proposed an approach for morphing structures and applied on a digital span-wise twist scenario, which they also performed wind-tunnel tests [11]. Vale et al. has investigated simultaneous twist and camber morphing wing design for roll control, drag minimization and active load alleviation [12]. Their study revealed a potential in roll control flight efficiency, and load alleviation improvement. Rodrigue et al. have performed a wind-tunnel experiment on a twist-morphing UAV made from smart soft composite, and obtained an improvement on aerodynamic performance [13].

In this study, the application of an innovative twist-morphing wing design was carried out on a ZANKA-I fixed-wing UAV with the aim of achieving the desired stall propagation together with improving autonomous flight performance in both lateral and longitudinal flight. The base model was redesigned with the capability of twisting the

wing in terms of wash-out angle between 0-degree to 6-degree. The longitudinal and lateral dynamic model of the aircraft mathematically constituted and aerodynamic, inertial and geometrical variations due to the morphing application were assessed. Meanwhile, benefiting from simultaneous design approach, the SPSA optimization algorithm was integrated to improve autonomous flight performance via adjusting controller parameters (i.e. PID coefficients) and washout angle. As a novel concurrent engineering approach, it is the first time in the literature evaluating wing-twist and control system simultaneously.

2 Material and methods

The base aerial vehicle model to be investigated in this manuscript is ZANKA-I fixed-wing UAV, whose detailed information could be achieved from the study by Oktay et al. [14]. In this section, firstly, the main philosophy and constraints of the twist-morphing design will be geometrically defined. The longitudinal and lateral dynamic model of the aircraft will be examined and the methodology on investigation of geometrical, inertial and aerodynamic effects of the morphing application will be determined. Moreover, the concurrent autonomous control system and wing design optimization approach will be described, together with simultaneous perturbation stochastic approximation (SPSA).

2.1 Twist-morphing wing design

The base aerial vehicle model has no washout applied to its main wing (with 1.3-meters span), as given in Figure 1a. The twist-morphing wing is designed to have washout angle ($\alpha_{washout}$) up to 6-degrees, which resulted in higher angle of attack at root section of the main wing as given in Figure 1b. In this scenario, the washout was obtained by angle of incidence variation at root section, and tip section's geometry was fixed.

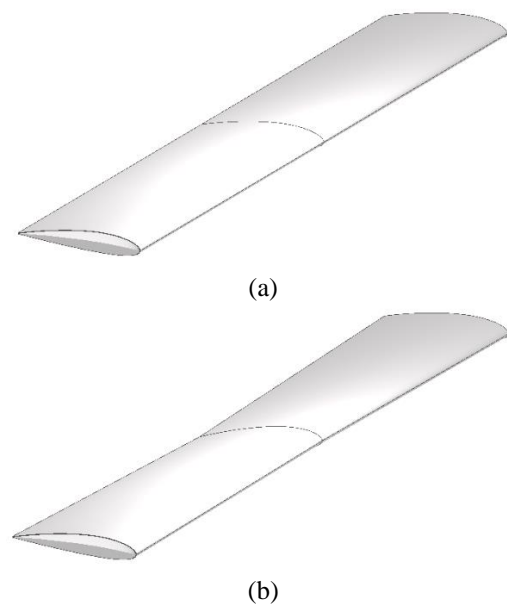


Figure 1. Twist-morphing wing design with (a) 0-degree washout angle (b) 6-degree washout angle [15]

2.2 Aircraft longitudinal and lateral dynamic model

The flight dynamics of an aerial vehicle could mathematically be defined as longitudinal and lateral dynamic models, which determines stability and control behaviors of the vehicle [16, 17].

Principally, the dynamic models include aircraft equations of motion defined as state variable representation as sets of first-order differential equations. Longitudinal and lateral dynamic models are given in Equation 1 and Equation 2, respectively. In the equations, x , y and z are the axes of aircraft frame of reference; u , v , and w , are linear velocities (m/s), p , q , and r , are angular velocities (rad/s), and θ , ϕ , and β are pitch, roll, and sideslip angles (rad), respectively. In addition, \dot{x} is the state vector, and u is the control vector, where A and B are the matrices include aircraft's stability and control derivatives, respectively. More details for the equations and included variables could be achieved from [17].

$$\begin{bmatrix} \Delta \dot{u} \\ \Delta \dot{w} \\ \Delta \dot{q} \\ \Delta \dot{\theta} \end{bmatrix} = \underbrace{\begin{bmatrix} X_u & X_w & 0 & -g \\ Z_u & Z_w & u_0 & 0 \\ M_u + M_{\dot{w}}Z_w & M_w + M_{\dot{w}}Z_w & M_q + M_{\dot{w}}u_0 & 0 \\ 0 & 0 & 0 & 0 \end{bmatrix}}_{A_{longitudinal}} \begin{bmatrix} \Delta u \\ \Delta w \\ \Delta q \\ \Delta \theta \end{bmatrix} + \underbrace{\begin{bmatrix} X_{\delta_T} & X_{\delta_e} \\ Z_{\delta_T} & Z_{\delta_e} \\ M_{\delta_T} + M_{\dot{w}}Z_{\delta_T} & M_{\delta_e} + M_{\dot{w}}Z_{\delta_e} \\ 0 & 0 \end{bmatrix}}_{B_{longitudinal}} \begin{bmatrix} \Delta \delta_T \\ \Delta \delta_e \end{bmatrix} \quad (1)$$

$$\begin{bmatrix} \Delta \dot{\beta} \\ \Delta \dot{p} \\ \Delta \dot{r} \\ \Delta \dot{\phi} \end{bmatrix} = \underbrace{\begin{bmatrix} \frac{Y\beta}{u_0} & \frac{Yp}{u_0} & -\frac{g}{u_0} \cos(\theta_0) & -(1-\frac{Yr}{u_0}) \\ L\beta^* + \frac{I_{xz}}{I_{xx}}N\beta^* & Lp^* + \frac{I_{xz}}{I_{xx}}Np^* & Lr^* + \frac{I_{xz}}{I_{xx}}Nr^* & 0 \\ N\beta^* + \frac{I_{xz}}{I_{zz}}L\beta^* & Np^* + \frac{I_{xz}}{I_{zz}}Lp^* & Nr^* + \frac{I_{xz}}{I_{zz}}Lr^* & 0 \\ 0 & 0 & 1 & 0 \end{bmatrix}}_{A_{lateral}} \begin{bmatrix} \Delta \beta \\ \Delta p \\ \Delta r \\ \Delta \phi \end{bmatrix} + \underbrace{\begin{bmatrix} 0 & \frac{Y\delta_r}{u_0} \\ L\delta_a^* + \frac{I_{xz}}{I_{xx}}N\delta_a^* & L\delta_r^* + \frac{I_{xz}}{I_x}N\delta_r^* \\ N\delta_a^* + \frac{I_{xz}}{I_{zz}}L\delta_a^* & N\delta_r^* + \frac{I_{xz}}{I_{zz}}L\delta_r^* \\ 0 & 0 \end{bmatrix}}_{B_{lateral}} \begin{bmatrix} \Delta \delta_a \\ \Delta \delta_r \end{bmatrix} \quad (2)$$

The variables of the dynamic models were dramatically affected from geometrical, aerodynamic and inertial variations. Thus, the variations driven by twist-morphing application should be investigated. Geometrical point of view, within such an application, occurs only angular an angular change, and aspect ratio and span of the wing stay constant. In addition, the inertial and aerodynamic assessment was numerically carried out in our previous conference paper and the obtained resultant values for various washout angles are given in Table 1 [15]. In order to obtain extended results for every washout angle between 0-

degree to 6-degree, a Nonlinear Least Squares (NLS) regression algorithm is also integrated [18].

2.3 Autonomous flight control system

The autonomous flight control system of ZANKA-I UAV has been presented in a previous study with conventional hierarchical structure composed of 6 PID (proportional, integral, derivative) controllers, where detailed information about the controller could be achieved from et al. [19]. The longitudinal and lateral controller PID coefficients of the system, which are proportional (k_p), integral (k_i), and derivative (k_d) dramatically known to affect the trajectory tracking performance of the aerial vehicle. For instance, the increasing values of k_r and k_l are known to result increment in maximum overshoot, while reduction in rise time. On the other hand, increasing value of k_d is known to result reduction in both maximum overshoot and settling time [20]. Therefore, these coefficients should be appropriately tuned during or pre-flight to obtain improved flight performance.

2.4 Simultaneous perturbation stochastic approximation (SPSA)

The flight dynamics (i.e. performance, stability and control) of an aircraft is a complex issue, as revealed in Equation 1 and Equation 2, commonly to be optimized aiming for various performance-based objectives. In that context, stochastic optimization methods have known to be flexible, adaptable and offering robustness to noise, on such complex problems rather than deterministic optimization methods (such as gradient-based methods, linear or quadratic programming, convex optimization etc.).

In this paper, the objective is to improve autonomous trajectory tracking performance of the aerial vehicle by means of 7 parameters, which are longitudinal and lateral PID coefficients together with wing washout angle. For that purpose, SPSA algorithm is preferred to be used as a gradient-free stochastic optimization algorithm that uses few numbers of recursion for loss-function evaluation. Theoretical background and detailed information about the SPSA methodology could be achieved from [21, 22].

In order to construct the cost-indexes, the longitudinal and lateral trajectory tracking performances of the aerial vehicle have defined in terms of rise time (T_{rt}), settling time (T_{st}) and maximum overshoot (OS). Longitudinal cost-index ($J_{longitudinal}$) and lateral cost-index ($J_{lateral}$) have summed to obtain total cost-index (J_{total}). Lateral cost-index is multiplied by weighing value of 100 to have similar impact on total cost-index as shown in Equation 3 and Equation 4.

$$J_{total} = J_{longitudinal} + J_{lateral} * (100) \quad (3)$$

$$J_{total} = (T_{rt} + T_{st} + OS)_{longitudinal} + (T_{rt} + T_{st} + OS)_{lateral} * (100) \quad (4)$$

The objective in our optimization case is to minimize the total cost-index to obtain improved trajectory tracking

performances for both 5-degree pitching and 5-degree roll flight scenarios at 16.66 m/s airspeed at sea-level conditions.

3 Results and discussions

3.1 Aerodynamic and inertial variations

The aerodynamic and inertial variations of the aerial vehicle obtained from 0-degree to 6-degree washout angles with 2-degree intervals as given in Table 1 [15].

Table 1. Aerodynamic and inertial variations with respect to washout angle

$\alpha_{washout}$	0°	2°	4°	6°
$I_{xx} (kgm^2)$	0.09878	0.09875	0.09871	0.09863
$I_{yy} (kgm^2)$	0.14219	0.14218	0.14199	0.14199
$I_{zz} (kgm^2)$	0.22971	0.22968	0.22962	0.22940
$I_{xz} (kgm^2)$	0.01276	0.0084	0.0040	0.0003
C_{D0}	0.01322	0.01107	0.00952	0.00864
C_{L0}	0.6494	0.4603	0.4256	0.3140
C_{La}	4.824	4.816	4.835	4.850
C_{Da}	0.1	0.08811	0.07551	0.06761
e	1.033	1.057	1.031	0.856

It is clear from the results that, zero-lift drag coefficient (C_{D0}) has been decreasing for whole washout angle interval, where reference lift coefficient (C_{L0}) has the similar tendency. Lift curve slope (C_{La}) and Oswald efficiency factor (e) point of view, washout application has been resulted in a polynomial behavior, which decreased/increased up to 2-degrees and increased/decreased at higher angles of washout. Drag curve slope (C_{Da}) point of view, completely decreasing trend was found for increasing washout angle applications.

Inertial parameters of the vehicle also varied with the twist-morphing application, where I_{xx} , I_{zz} and I_{xz} has a decreasing trend with increasing values of washout angle. I_{yy} has found to vary similar with lift-curve slope and has polynomial behavior.

The results of such a complex behavior of foresaid parameters with twist-morphing application dramatically affects the dynamic model of the vehicle given in Equation 1 and Equation 2. The effects of the variation in washout angle on stability and control derivatives of the aerial vehicle was presented in our previous conference paper and could be achieved from [15].

3.2 SPSA optimization

The nonlinear variation in emphasized parameters dramatically affects the performance of longitudinal and lateral dynamic models, and should be optimized with an appropriate methodology, which is determined as SPSA in this study. In that context, the simultaneous design approach comes to the fore and the estimation of the most proper washout angle together with longitudinal and lateral PID coefficients is essential. In summary, the application refers to concurrent design of aircraft wing and control system. In this regard, the obtained aerodynamic and inertial data used for regression analyses and expanded via NLS algorithm in MATLAB environment and linked to constituted aircraft dynamic models.

The SPSA algorithm was adjusted to optimize both wing design and control system to obtain a successful trajectory tracking in terms of 5-degree pitching motion and 5-degree rolling motion. Initial values of PID coefficients and washout angle, which the base model have, are 50, 5, 50 and 0-degree, respectively. Correspondingly, the initial values for longitudinal, lateral and total costs are given in Table 2.

The results of the optimization using SPSA were found to be converged after a few iterations, as expected, shown in Figure 2. The decrement in cost index implies improvement in trajectory tracking qualities defined in the sum of maximum overshoot, rise time, and settling time in Equation 4. Accordingly, trajectory tracking performance point of view, longitudinal and lateral flight performances were found to increase by 33.92% and 33.81% with respect to the initial design, respectively. Moreover, the total flight performance of the aircraft was found to increase by 65.14% as summarized in Table 2.

Table 2. Base and optimized values of longitudinal, lateral and total costs

Variable	Initial value	Optimized value	Difference
$J_{longitudinal}$	0.6634	0.4383	-33.92%
$J_{lateral}$	0.000364	0.000240	-33.81%
J_{total}	1.326	0.4624	-65.14%

In Table 3, the initial and optimized values of PID coefficients and washout angle are given. The results shown the tendency of the algorithm to decrease the proportional and integral coefficients and increase the derivative coefficient for both longitudinal and lateral cases. Correspondingly, the change in such parameters has an effect on trajectory tracking parameters of rise time, settling time and overshoot, whose initial and optimized values were summarized in Table 4. For lateral case, maximum overshoot has found not to be changed as it was initially having optimal value. In addition, settling time has found to be considerably decreased due by means of decrement in integral coefficient. For longitudinal case, the increase in the derivative coefficient has found to be resulted in a substantial decrement of maximum overshoot, as expected. Also settling time has found to be increased, and maximum overshoot has found to be decreased due to the dramatical increment in derivative coefficient.

Table 3. Base and optimized values of PID coefficients

Variable	Initial value	Optimized value
$k_{plongitudinal}$	50	27.50
$k_{llongitudinal}$	5	2.51
$k_{Dlongitudinal}$	50	74.88
$k_{plateral}$	50	27.38
$k_{llateral}$	5	2.51
$k_{Dlateral}$	50	74.99
Washout angle	0 (degree)	2.2 (degree)

In Figure 3, the variation of longitudinal and lateral PID coefficients with respect to iteration index were presented, which clearly represents a convergence after few iterations.

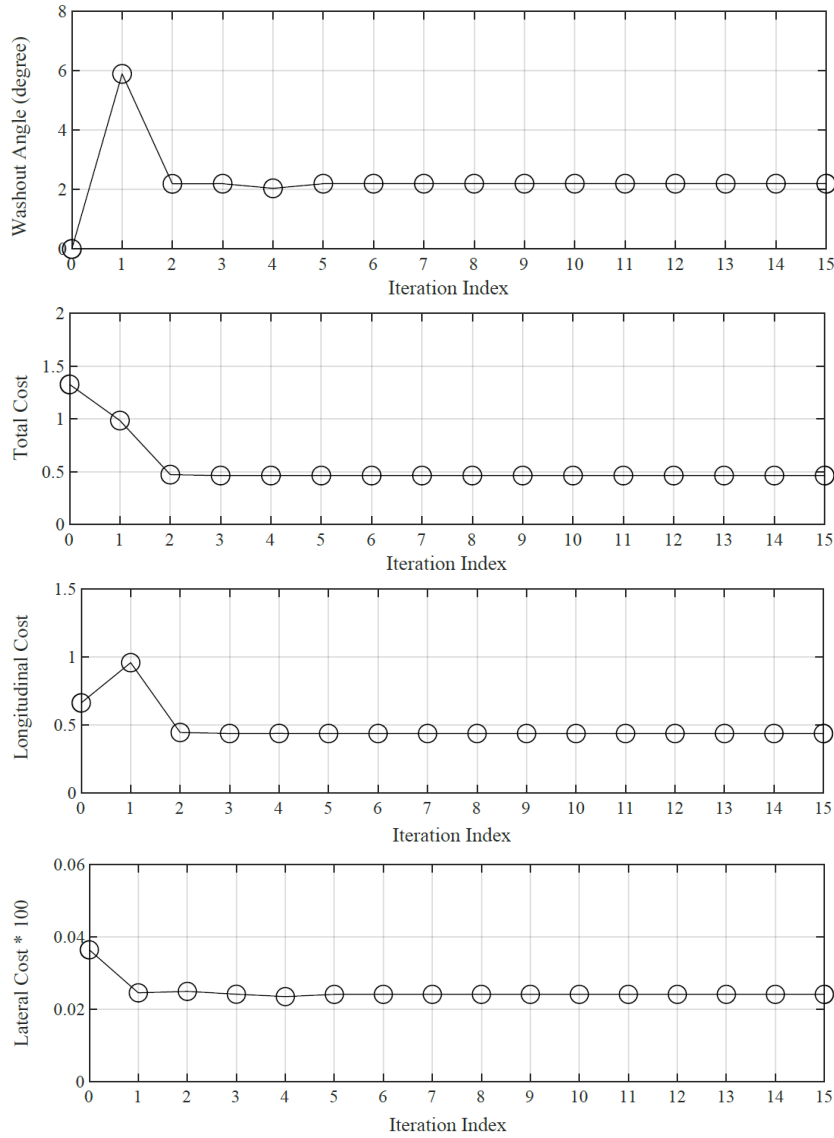


Figure 2. The convergence of longitudinal, lateral and total costs and washout angle with iteration index

Table 4. Base and optimized values of trajectory tracking parameters and percentage difference

Variable	Initial value	Optimized value	Difference
$Trt_{longitudinal}$	0.04037	0.02495	-38.19%
$TSt_{longitudinal}$	0.33329	0.43751	+31.27%
$OS_{longitudinal}$	0.28974	0	-100%
$Trt_{lateral}$	0.0001300	0.0000862	-33.65%
$TSt_{lateral}$	0.0002341	0.0001547	-33.9%
$OS_{lateral}$	0	0	-

In summary, the only loss obtained among the parameters has found as the longitudinal settling time, which has found to be increased by 31.27%. Nonetheless, in total, the trajectory tracking performance of the vehicle has been found to be increased by 65.14%, which means a remarkable improvement. Geometrical point of view, the washout angle of the twist-morphing main wing has found to be applied as 2.2 degrees that provides a desired stall propagation beginning from the root section.

Aerodynamic point of view, drag coefficient of an aircraft is the sum of induced (C_{Di}) and zero-lift drag coefficients, and the induced drag could be achieved from Equation 5. As the aspect ratio (AR) of the wing is constant, the decrement in lift coefficient and increment in Oswald efficiency results a great decrement in induced drag of the vehicle.

$$C_{D_i} = \frac{C_L^2}{\pi e AR} \quad (5)$$

On the other hand, the decrement in aerodynamic performance (L/D) results a decrease in range (R) of the aircraft, as given in Equation 6, where η is the propulsive efficiency, C is the specific fuel consumption and W_0 and W_1 are the initial and final weights of the aircraft, respectively.

$$R = \frac{\eta}{C} \frac{C_L}{C_D} \ln \left(\frac{W_0}{W_1} \right) \quad (6)$$

Stall speed of the vehicle stays constant with the change in washout angle as the maximum lift coefficient and wing area (S) is constant, as given in Equation 7.

$$V_{STALL} = \sqrt{2\rho S C_{L_{MAX}}} \quad (7)$$

Flight performance point of view, the takeoff distance of the vehicle has not been affected remarkably, where the propulsive forces are dominant than aerodynamic forces. In case of landing, the landing distance could be slightly increased with respect to the decrement in drag force. In cruise flight, decrement in lift coefficient could require to cruise at a higher airspeed to preserve the flight altitude,

where weight force of the vehicle should be equal to produced lift force as given in Equation 8.

$$W = \frac{1}{2} \rho S V^2 C_L \quad (8)$$

4 Conclusions

In this paper, an innovative twist-morphing wing design has been applied on a fixed-wing unmanned aerial vehicle to obtain an improvement in autonomous flight performance (i.e. trajectory tracking performance). The main wing was redesigned with the capability of morphing to have a washout angle between 0-degree to 6-degree, which differs root and tip sections of the wing to adjust the stall propagation as desired. In that context, the simultaneous design approach was applied for wing and control system design to obtain trajectory tracking performance enhancement.

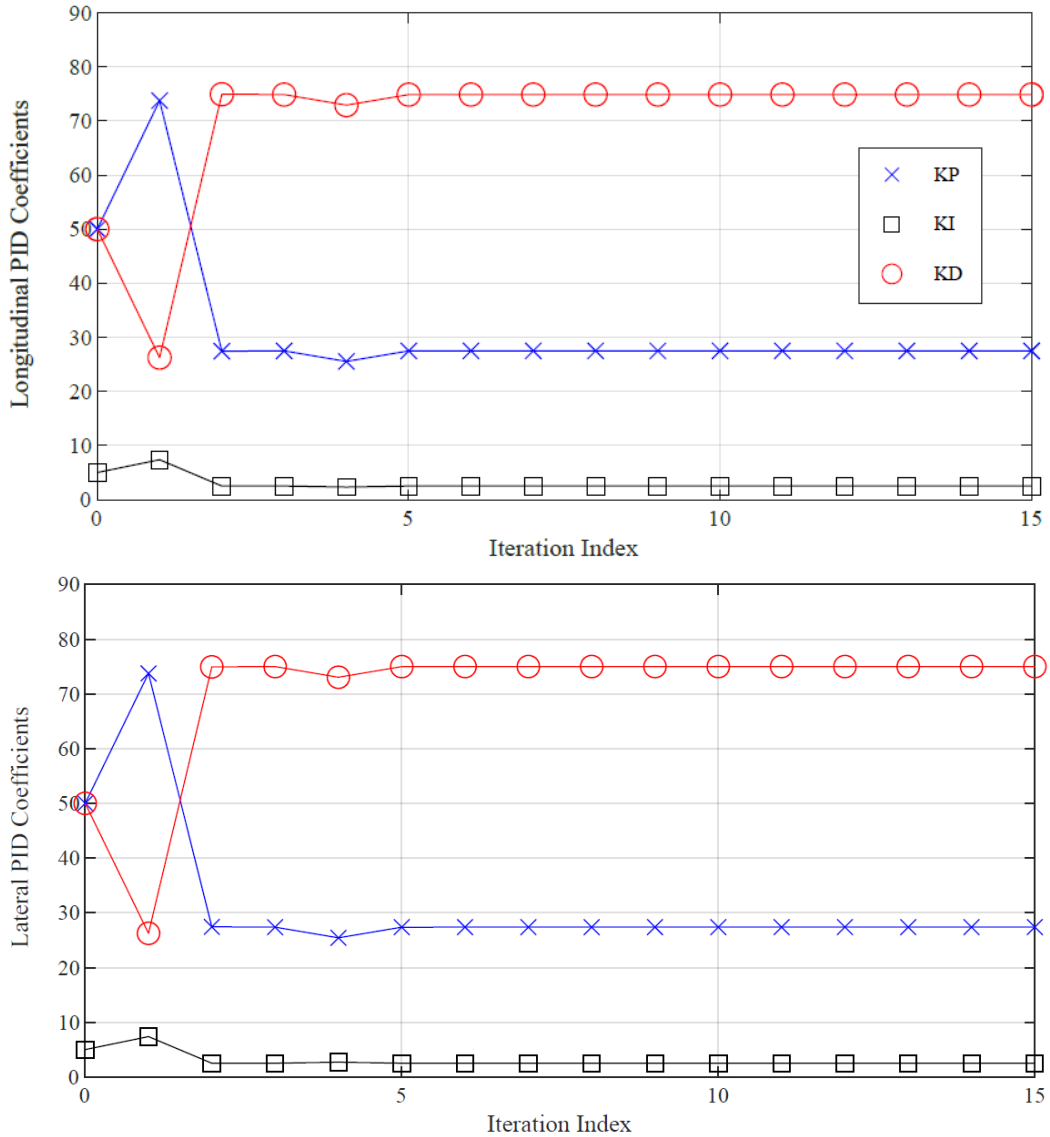


Figure 3. The convergence of longitudinal and lateral PID coefficients with iteration index

For that purpose, the constituted dynamic models of the vehicle integrated into the SPSA optimization algorithm, which is empowered with conduction of NLS algorithm. Control system parameters (i.e. PID coefficients) and washout angle (i.e. totally 7 parameters) were estimated by the algorithm aiming for improvement in trajectory tracking performances defined in terms of rise time, settling time and maximum overshoot for both longitudinal and lateral flights.

The simultaneous design approach has resulted in an improvement in total performance by 65.14%, while 33.92% and 33.81% in longitudinal and lateral trajectory tracking performances, respectively. Consequently, initial main wing geometry has redesigned to have 2.2-degree washout angle and improved also in terms of stall propagation. In conclusion, this study has clearly shown the potential behind the simultaneous design approach on aircraft design processes and various morphing ideas.

As a future work, the proposed concurrent design methodology could be applied not only for control system and aerodynamic designs, it could be useful for various disciplines such as propulsion and structural design issues. The combination of different disciplines could be benefited for aircraft conceptual and preliminary designs and pave the way for developing novel applications in aircraft design.

Nomenclature

x, y, z - positions along x, y and z axes;
 u, v, w - linear velocities along $x, y,$ and z axes;
 p, q, r - roll, pitch and yaw rate;
 X, Y, Z - forces along $x, y,$ and z axes;
 L, M, N - moments about $x, y,$ and z axes;
 I_{xx}, I_{yy}, I_{zz} - moments of inertia about $x, y,$ and z axes;
 I_{xz} - moment of inertia about xz -plane;
 $\delta_r, \delta_e, \delta_a$ - deflection of rudder, elevator and aileron;
 $\psi, \theta, \phi, \beta$ - yaw, pitch, roll and sideslip angles.

Acknowledgment

A part of this paper is presented in Avrasya 10th International Conference on Applied Sciences on May 2-5 2024, Tbilisi, Georgia [15].

Conflict of interest

The authors declare that there is no conflict of interest.

Similarity rate (iThenticate): %17

References

- [1] S. Ameduri and A. Concilio, Morphing wings review: Aims, challenges, and current open issues of a technology. Proceedings of the Institution of Mechanical Engineers, Part C: Journal of Mechanical Engineering Science, 237(18), 4112-4130, 2023. <https://doi.org/10.1177/0954406220944423>
- [2] K. Sharma and G. Srinivas, Flying smart: Smart materials used in aviation industry, Materials Today: Proceedings, 27, 244-250, 2020. <https://doi.org/10.1016/j.matpr.2019.10.115>
- [3] R. M. Ajaj, M. S. Parancheerivilakkathil, M. Amoozgar, M. I. Friswell and W. J. Cantwell, Recent developments in the aeroelasticity of morphing aircraft, Progress in Aerospace Sciences, 120, 100682, 2021. <https://doi.org/10.1016/j.paerosci.2020.100682>
- [4] A. Dharmdas, A.Y. Patil, A. Baig, O.Z. Hosmani, S.N. Mathad, M.B. Patil, R. Kumar, B.B. Kotturshettar and I.M.R. Fattah, An Experimental and simulation study of the active camber morphing concept on airfoils using bio-inspired structures. Biomimetics, 8(2), 251, 2023. <https://doi.org/10.3390/biomimetics8020251>
- [5] B.W. Jo and T. Majid, Enhanced range and endurance evaluation of a camber morphing wing aircraft. Biomimetics, 8(1), 34, 2023. <https://doi.org/10.3390/biomimetics8010034>
- [6] T. Oktay and Y. Eraslan, Impacts of tapered wingtip on lateral-directional stability coefficients of a morphing fixed-wing UAV. The Black Sea Journal of Sciences, 13(4), 1540-1551, 2023. <https://doi.org/10.31466/kfbd.1309152>
- [7] L. Gao, Y. Zhu, X. Zang, J. Zhang, B. Chen, L. Li and J. Zhao, Dynamic analysis and experiment of multiple variable sweep wings on a tandem-wing MAV. Drones, 7(9), 552, 2023. <https://doi.org/10.3390/drones7090552>
- [8] E. Kaygan and C. Ulusoy, Effectiveness of twist morphing wing on aerodynamic performance and control of an aircraft. Journal of Aviation, 2(2), 77-86, 2018. <https://doi.org/10.30518/jav.482507>
- [9] N. I. Ismail, M.A. Tasin, H. Sharudin, M.H. Basri, S.C. Mat, H. Yusoff and R.E.M. Nasir, Computational aerodynamic investigations on wash out twist morphing MAV wings. Evergreen, 9(4), 1090-1102, 2022. <https://doi.org/10.5109/6625721>
- [10] A. Gatto, Development of a morphing UAV for optimal multi-segment mission performance. The Aeronautical Journal, 127(1314), 1320-1352, 2023. <https://doi.org/10.1017/aer.2022.99>
- [11] B. Jenett, S. Calisch, D. Cellucci, N. Cramer, N. Gershenfeld, S. Swei and K.C. Cheung, Digital morphing wing: active wing shaping concept using composite lattice-based cellular structures. Soft robotics, 4(1), 33-48, 2017. <https://doi.org/10.1089/soro.2016.0032>
- [12] J. Lobo do Vale, J. Raffaelli and A. Suleman, Experimental validation and evaluation of a coupled twist-camber morphing wing concept. Applied Sciences, 11(22), 10631, 2021. <https://doi.org/10.3390/app112210631>
- [13] H. Rodrigue, S. Cho, M.W. Han, B. Bhandari, J.E. Shim and S.H. Ahn, Effect of twist morphing wing segment on aerodynamic performance of UAV. Journal of Mechanical Science and Technology, 30, 229-236, 2016. <https://doi.org/10.1007/s12206-015-1226-3>
- [14] T. Oktay, M. Konar, M. Onay, M. Aydin and M.A. Mohamed, Simultaneous small UAV and autopilot system design. Aircraft Engineering and Aerospace Technology, 88(6), 818-834, 2016. <https://doi.org/10.1108/AEAT-04-2015-0097>
- [15] Y. Eraslan and T. Oktay, Stability assessment of unmanned aerial vehicle with twist-morphing wing.

- Avrasya 10th International Conference on Applied Sciences, p. 88-95, Tblisi, Georgia, May 2-5 2024.
- [16] J. Roskam, Airplane Flight Dynamics and Automatic Flight Controls. DARcorporation, USA, 1998.
- [17] R.C. Nelson, Flight Stability and Automatic Control. WCB/McGraw Hill, New York, 1998.
- [18] T. Oktay and Y. Eraslan, Autonomous flight performance optimization of fixed-wing unmanned aerial vehicle with morphing wingtip. Aircraft Engineering and Aerospace Technology, 96(3), 475-482, 2024. <https://doi.org/10.1108/AEAT-09-2022-0262>
- [19] Y. Eraslan, and T. Oktay, Multidisciplinary Performance Enhancement on a Fixed-wing Unmanned Aerial Vehicle via Simultaneous Morphing Wing and Control System Design. Information Technology and Control, 52(4), 833-848, 2023. <https://doi.org/10.5755/j01.itc.52.4.33527>
- [20] A. Baharuddin and M.A.M. Basri, Trajectory Tracking of a quadcopter UAV using PID controller. ElektriKA-Journal of Electrical Engineering, 22(2), 14-21, 2023. <https://doi.org/10.11113/elektrika.v22n2.440>
- [21] J.C. Spall, Multivariate stochastic approximation using a simultaneous perturbation gradient approximation. IEEE Transactions on Automatic Control, 37, 1992.
- [22] I. J. Wang, and J.C. Spall, Stochastic optimisation with inequality constraints using simultaneous perturbations and penalty functions. International Journal of Control, 81(8), 1232-1238, 2008. <https://doi.org/10.1080/00207170701611123>

